J. Coat. Technol. Res., **15** (1) 51–64, 2018
DOI 10.1007/s11998-017-9945-2

Fabrication of superhydrophobic coatings for combating bacterial colonization on Al with relevance to marine and medical applications

R. Mohan Raj, V. Raj

Abstract Aluminum and its alloys are widely used in almost all industries and for marine and medical applications. However, their surfaces are easily colonized by bacteria that form biofilms and corroded by chemical reactions. We report here a simple method to fabricate polyaniline/chitosan/zinc stearate superhydrophobic coatings on aluminum with a micro–nanosurface structure by polymerization of aniline and deposition of chitosan and zinc stearate coating. The fabricated coatings have been characterized by ATR-IR, XRD, FE-SEM, and EDX. The superhydrophobic surface shows the highest water-repellent property with contact angle of 150.7°, which is responsible for antiadhesion of bacteria, antiicing property, and excellent corrosion resistance of aluminum. The corrosion behavior of the coating in the 3.5% NaCl solution was investigated by EIS and potentiodynamic polarization. The efficacies of the different coatings against bacteria that are commonly encountered in marine (*Desulfovibrio desulfuricans*) and medical applications (*Staphylococcus aureus* and *Escherichia coli*) are demonstrated.

Graphical Abstract

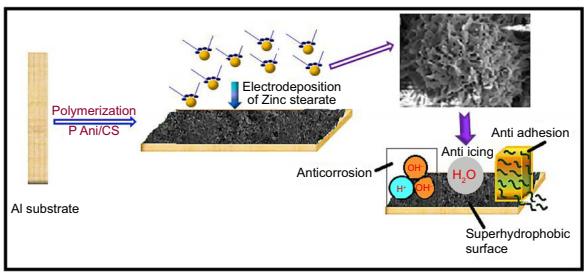

R. Mohan Raj, V. Raj (✉)
Advanced Materials Research Laboratory, Department of Chemistry, Periyar University, Salem 11, Tamil Nadu, India
e-mail: alaguraj2@rediffmail.com

R. Mohan Raj
e-mail: chem_mohan@rediffmail.com

Keywords Aluminum, Bacterial adhesion, Biofilms, Superhydrophobic coating, Corrosion resistance

Introduction

Aluminum (Al) possesses a very low density and is widely used in daily life, which includes the aerospace, construction, packaging, shipping, and transportation industries, and on household items. Unfortunately, Al itself does not have antibacterial activity, and microorganisms easily breed on the Al surface. It was reported that the trouble caused by microorganisms on the parts of precise apparatus of spaceflight[1] is called microbiologically influenced corrosion (MIC) or biocorrosion.[2–4] Biocorrosion is extremely dangerous to aquatic, maritime, and process industries, as well as to the environment.

In addition to the economic losses, the existence and breeding of microorganisms on the surface of Al products will cause industrial problems. These biofilms pose a hygiene risk in the food industry and increase the risk of infections in the medical field.[5] In both marine and biomedical applications, metals play a very important role. Modification of the surface of the metals makes them resistant to bacterial colonization in marine and medical applications. These techniques centered on the use of polymers that are antiadhesive and/or bactericidal. The polymer coatings are correspondingly tailored to meet the specific challenges.[6,7]

There are countless studies that have examined for the utilization of conducting polymers (CPs) as protective coatings against corrosion, because of their relatively high environmental stability and nontoxic, simple, and economical production routes.[8] Among the CPs, PAni has been explored widely by the researchers for the protection of metals.[9,10] Nagels et al.,[11] Sekine et al.,[12] and Kamaraj et al.[13] have shown that the electropolymerized PAni films alone on metal do not satisfactorily protect the surface against corrosion. The use of PAni in technolog-

ical applications is hampered by its poor processibility, related to low solubility in common solvents. This problem of nonprocessibility of PAni can be tackled by copolymerization of aniline with other polymers.[14,15]

Chitosan (CS) is one of the most promising polysaccharides due to its antimicrobial activity, biodegradability, and excellent film-forming ability, and hence, it has been used in several fields such as biotechnology, biomedicine, cosmetics, pharmaceuticals, packaging, wastewater treatment, and food science.[16,17] CS polymer provides small barrier effect, so additional active corrosion protection is required to ensure an effective suppression of the corrosion processes on the metal surface. CS/PAni coatings exhibit much better protection behavior than single CS coatings.

The stability of coating constitutes an important matter for outdoor applications or severe conditions. In order to develop better coatings, numerous methods have been dealing with the modification of polymer coatings.[18–20] The zinc/zinc oxide layer behaves like a sacrificial anode against the corrosion of metal, and the organic coatings layer constitutes a physical barrier between the corrosive environment and the substrate. In addition, zinc has been shown to exhibit antimicrobial properties, useful for hospital and food processing applications.[21] Recently, superhydrophobic coatings have been applied to various material surfaces such as steel, copper, zinc, and aluminum, to improve their corrosion resistance performances.[22–24] Superhydrophobic surfaces give rise to certain applicative properties, such as self-cleaning, antiicing, antifouling, corrosion resistance, and oil/water separation.[25] Traditionally, superhydrophobic surfaces are made by combining rough micro–nanosurface and the passivation of the rough surface using a low surface energy coating. These combined effects of air entrapment in the rough micro–nanostructures and the low surface energy reduces the affinity of water toward the surface.[26–28]

This study aims at investigating the effect of polymer coatings on the surface morphology and corrosion resistance of optimized polymer coating and zinc stearate (ZS) superhydrophobic coating. The corrosion behavior was analyzed by potentiodynamic polarization and EIS methods in 3.5 wt% NaCl solution. Finally, modified superhydrophobic Al substrate is subjected to biofilm formation, and antibacterial performance study was conducted against microalgae adhesion. The advantages shown with the present study include cheap and fluorine-free raw materials, environmentally friendly properties, and feasibility for applying an large area on different substrates.

Experimental

Materials

All the chemicals used in this work were of analytical grade, purchased from Sigma-Aldrich, and used without further purification. All the electrolytes and reagents were prepared using double-distilled water.

Formation of PAni/CS

The annealed Al foil was used as starting material. A preliminary treatment was performed in which Al foils were degreased with acetone, alkali cleaned with 5% NaOH at 30°C for 2 min followed by desmutting in 25% HNO_3 at 30°C for 1 min. The pretreated Al specimen was subjected to a polymerization process. An electrolyte of 0.1 M sulfuric acid with various concentrations of aniline (0.1–0.3 M) with and without the addition of CS (0.5–1.5%) was used for electrosynthesis of PAni and PAni/CS coatings on Al. The polymerization was carried out using a two-electrode configuration connected to a DC power supply with Al foil as anode having the working area of about 1 cm^2 and graphite as cathode in a thermostatically controlled setup.[29]

In order to investigate the influence of electrolytes on polymerization coatings, the polymerization was conducted on two different electrolytes: (1) various concentrations of aniline (0.1–0.3 M) in 0.1 M H_2SO_4 and (2) various concentrations (0.5–1.5 W/V %) of CS in 1% acetic acid with optimized concentrations of aniline. The applied voltage was fixed at 16 V. The polymerization coatings were fabricated from both electrolytes with stirring at room temperature for 30 min. After polymerization, the specimen was washed with distilled water and dried.

Fabrication of PAni/CS/ZS coating

Optimized PAni/CS-coated Al plates were taken as the cathode and lead as an anode in an electrolytic cell, and DC voltage was applied to the two electrodes separated at a distance of 2.0 cm to deposit zinc stearate coating. The electrolyte used was 100 ml ethanol solution of $Zn(NO_3)_2$ (0.10 M) and stearic acid (0.20 M). The electrodeposition was conducted at room temperature by applying DC voltage of 5 V for 15 min. After deposition, the plate was rinsed with distilled water and dried at ambient temperature for the subsequent characterization.

Characterization of the fabricated coatings

The PAni/CS polymer coating and the PAni/CS/ZS coating were characterized by ATR-IR (Bruker–Tensor 27), over the wavelength range from 4000 to 400 cm^{-1}. The crystallographic characteristics of the coatings were investigated with X-ray diffractometer (XRD, X-pert Graphics, Brooker, Germany) working in Cu K radiation. The surface morphology of the as-formed coatings

was examined by scanning electron microscope (SEM, FEI—QUANTA–FEG 250, Japan). All the samples were sputtered with thin gold film before SEM analysis to prevent surface charging effects.

Thickness of the coating was evaluated using a Dermitron thickness tester. The thickness values were measured in three different places in the specimen, and the average value was taken. The thickness value was divided by treatment time in minutes to get the growth rate. The unit of the growth rate is μm/min. Microhardness was measured using Automatic microhardness tester HV 1000B (Acme Engineers, Pune) at 25 g load and 10 s dwell time. For assessing the adhesion of the coating on Al substrate, a standard test method (Scotch Tape method, ASTM D 3359-02) was used. The abrasion resistance of the coatings was measured as per ASTM D 4060 method tested at 1 kg load using SiC wheels at 100 cycles using Montel Rotary Abrasion tester (Caltech Engineering Services, Mumbai).

Surface wettability of the coatings was tested using a video-based contact angle meter (OCA 15EC, Data Physics Instruments, Germany). Five measurements were taken at different locations of solid specimen, and an average contact angle was calculated. The ice adhesion force was calculated from the rotation speed at which ice detached from the specimens. Ice adhesion strength is assumed to be equal to the centrifugal force $(F) = mr\omega^2$, where m is the ice mass, r is the beam radius, and ω is the rotation speed (rad s^{-1}). From the F value, shear stress is calculated as $= F/A$. The roughness of the resulting samples was measured employing a surface roughness measuring instrument (HOMMEL-ETAMIC W10, Germany).

The surface energy was calculated according to the Owens–Wendt (OW) method given by[30,31]

$$(1 + \cos\theta)\gamma L = 2\left(\gamma L^d + \gamma S\gamma^d\right) + \left(\gamma L^p + \gamma S^p\right) \quad (1)$$

$$\gamma S = \gamma S^d + \gamma SP \quad (2)$$

where θ is the contact angle, γ is the surface energy, the subscripts L and S stand for liquid and solid, respectively, and the superscripts d and p represent the dispersive component and polar component. The surface energy, dispersive component, and polar component for distilled water are 72.8 mJ/m^2, 21.8 mJ/m^2, and 51.0 mJ/m^2, and those for ethylene glycol are 48.0 mJ/m^2, 29.0 mJ/m^2, and 19.0 mJ/m^2, respectively.

The corrosion resistance of various coatings was evaluated by electrochemical impedance spectroscopy and Tafel polarization studies. The corrosion studies were carried out in 3.5% NaCl at 30°C using electrochemical workstation (CHI Instruments, 760 model). A three-electrode cell with various coated aluminum as working electrode, Ag/AgCl/saturated KCl as reference electrode, and a platinum wire as counter-electrode were used. The potentiodynamic polarization studies were carried out at a potential range from −1200 to 200 mV vs. SCE for various coatings on Al samples. The electrochemical impedance spectroscopy (EIS) measurements were taken in the 0 MHz to 500 kHz frequency range using a 5 mV amplitude perturbation. All the measurements were recorded using internally available software, and each electrochemical experiment was repeated at least three times to ensure the reproducibility. All the experiments were conducted in aerated and nonstirred conditions. In order to obtain accurate results, the experiments were repeated in triplicate.

Antimicrobial studies

The two bacterial strains *S. aureus* (ATCC 25923) and *E. Coli* (ATCC 25922) were used to study the in vitro antimicrobial properties of the PAni, PAni/CS, PAni/CS/ZS coatings on Al substrate using the agar disk diffusion technique. The inoculums of the microorganisms were prepared from fresh overnight broth cultures (Tryptic soy broth with 0.6% yeast extract) that were incubated at 37°C. The agar disk diffusion test was performed at Muller-Hinton agar. The diffusion technique was carried out by pouring agar in petri dishes to form 4-mm-thick layers and adding dense inoculua of the test organisms of two bacterial strains in order to obtain better growth. Petri plates were left for 10 min in the laminar air flow, and after that, the disks were immersed into 50 μl of the as-developed coating powders. Then the disks were placed at equal distance and incubated for 24 h at 37°C. The width of the zone of inhibition (mm) around the disk, which was produced by the coatings against the two bacterial strains, was measured.

Marine bacterial studies

The marine bacteria used in this study were the sulfate-reducing strains of *Desulfovibrio desulfuricans* (ATCC#14563). The bacterium was cultured at 37°C in a modified Postgate's C medium used for enrichment culture, which contained 35 g NaCl, 0.5 g KH_2PO_4, 0.06 g $CaCl_2{\cdot}6H_2O$, 2 g $MgSO_4{\cdot}7H_2O$, 1 g yeast extract, 0.004 g $FeSO_4{\cdot}7H_2O$, and 0.3 g sodium citrate in 1 L deionized water. The medium was autoclaved at 121°C and 20 psi for 15 min.[32] After the stipulated time period (7 days), the various coated samples were washed twice with phosphate-buffered saline (1× PBS, pH 7.4). The cells were detected by live/dead staining. 200 μL of dye mixture (100 μL acridine orange, green fluorescence in live cells, and 100 μL ethidium bromide, red fluorescence in dead cells in distilled water) was mixed with 2 ml cell suspension in well plate. The suspension was immediately examined and viewed under Olympus inverted fluorescence microscope (Ti-Eclipse) at 200× and 400× magnification.

Results and discussion

Optimization of PAni coatings

The polymerization was carried out in 0.1 M H_2SO_4 containing various aniline concentrations from 0.1 to 0.3 M and applied voltage of 16 V at room temperature for 30 min, and their effect on formation of PAni coating was studied. In this bath, maximum thickness (23.0 μm) and growth rate (0.56 μm/min) for the PAni coating are obtained from 0.2 M concentration of aniline at 16 V. As the concentration of aniline increases, polymerization takes place gradually and growth of PAni film increases. The properties of the coating, such as thickness and growth rate, increase to a certain level, i.e., up to 0.2 M. Beyond that, the properties decrease as shown in Figs. 1a and 1b. The reason for this may be explained as follows. When the concentration of aniline is greater than 0.2 M, the pH of the solution decreases, as more amounts of H^+ ions is generated and it reduces the pH. At this low pH, instead of oxidation of monomer, Al substrate dissolves predominantly.[33,34] As a result, the formation of PAni coating decreases, and so, the thickness and growth rate decrease. From this, optimum concentration of aniline is found to be 0.2 M.

Optimization of PAni/CS coatings

PAni/CS coating was fabricated by polymerization in the bath containing 0.1 M H_2SO_4 and 0.2 M aniline optimized concentration and varying concentrations of CS solutions at applied voltage 16 V. In this bath, maximum thickness (29.1 μm) and growth rate (0.745 μm/min) are obtained for PAni/CS coatings at 0.15% (W/V) of CS with 0.2 M aniline. As the concentration of CS increases, the properties of thickness and growth rate of the coating increase to a certain level up to 0.15% (W/V) of CS. Beyond that, the coating properties decrease as shown in Figs. 1a, and 1b. The reason for this is explained as follows. CS possesses a high charge density. While adding CS in 0.2 M aniline, hydrogen bonds formed between them reduce the positive charge density and form a homogeneous phase, thereby increasing the mass. These interactions will increase the stability of the polymer film. The properties such as rate of film growth and thickness increase with increase in concentration of CS. On the contrary, when the concentration of CS was further increased to 0.20% (W/V), there is an electrostatic repulsion between CS and PAni, so that the quantity of the deposition of CS particles decreases and increases the monomer viscosity that also decreases the thickness and growth rate. So, the optimum concentration of CS for formation of a better quality coating is 0.15% (W/V) in 1% acetic acid.[35]

Mechanism PAni/CS/ZS coatings

The optimized PAni/CS coating has number of nitrogen atoms in the amino and N-acetyl amino groups, which can establish dative bonds with transition metal ions.[36] Zn^{2+} ion coordinated first with N-atom present on PAni/CS, and then self-assembled monolayers of stearic acid are formed on the Zn^{2+} with PAni/CS surface easily. We presume that Zn^{2+} ions are released continuously from $Zn(NO_3)_2$ into the stearic acid solution according to equations (3) and (4).

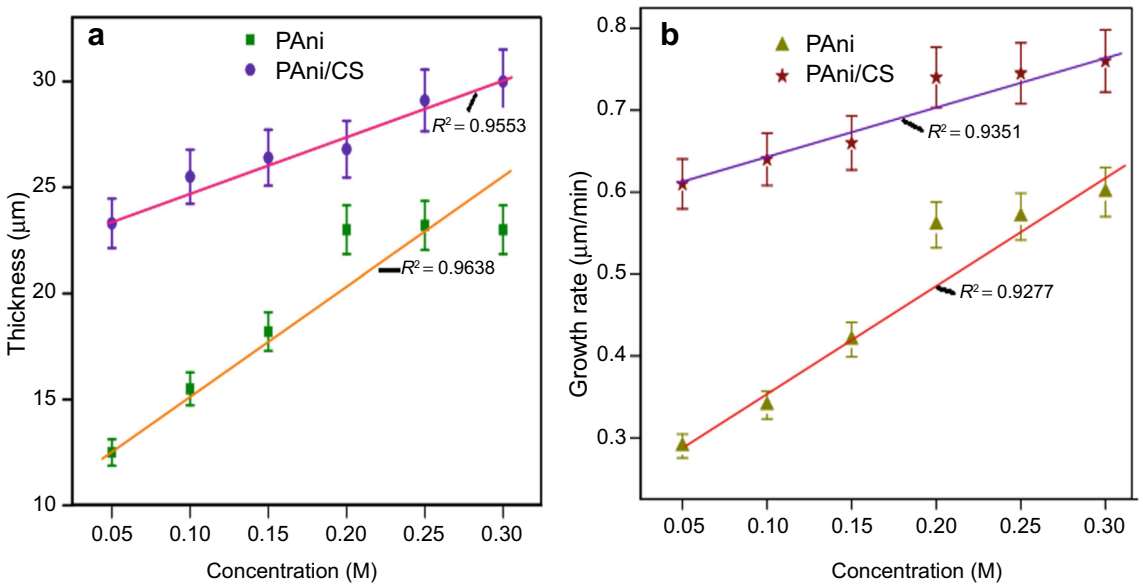

Fig. 1: Effect of aniline and CS concentration. (a) Thickness. (b) Growth rate

$$2Zn(NO_3)_2 \rightarrow 2Zn^{2+} + 2NO_3^- . \quad (3)$$

$$Zn^{2+} + 2CH_3(CH_2)_{12}COO^{2-} \rightarrow Zn\left[CH_3(CH_2)_{12}COO\right]_2 + 2H^+ . \quad (4)$$

Characterization of the fabricated coatings

FTIR spectral analysis

The FTIR spectra of PAni, PAni/CS and PAni/CS/ZS coatings formed on Al are shown in Figs. 2a to 2c. In the IR spectrum of PAni (Fig. 2a), the peak at 3415 cm^{-1} is related to N–H stretching vibration. The peaks at 1618 cm^{-1} and 1494 cm^{-1} are attributed to quinoid and benzenoid ring vibrations of PAni. The vibration of N=Q=N has characteristic absorption at 1105 cm^{-1}, and the peak in the region at 504–739 cm^{-1} is due to C–H bending vibration of substituted benzene ring.[37]

In the IR spectrum of CS/PAni (Fig. 2b), the peak at 3415 cm^{-1} is due to overlapping between O–H stretching vibration in CS and N–H stretching vibration in PAni (H-bond interaction). The peak at 2919 cm^{-1} is due to C–H stretching vibration of CS. The peak at 1553 cm^{-1} belongs to C=C stretching vibration in quinoid rings of PAni, and the peak at 1521 cm^{-1} is due to stretching vibrations in benzenoid rings of PAni. The peak at 1397 cm^{-1} is due to C–OH vibration of alcohol group in CS. The peak at 1101 cm^{-1} belongs to antisymmetric stretching of C–O–C bridge in CS. The peak at 3435 cm^{-1} is due to H-bonding interaction between PAni and CS, that is –OH and $–NH_2$.[38] FTIR results suggest that there is an interaction between aniline and active sites of CS.

The IR spectrum of the CS/PAni/ZS coating shows (Fig. 2c) the absorption band at 520 cm^{-1} which is typical Zn–O–Zn bond.[39] In the low-frequency region, the peak at 1701 cm^{-1} is attributed to the carboxyl group in stearic acid and it is present in the PAni/CS/ZS coating. A new absorption peak at 1596 cm^{-1} arises from the coordinated COO^- group and is found in the spectrum of the superhydrophobic coating.[40] These results indicate that the chemical reaction between carboxyl groups in stearic acid and Zn–OH at the PAni/CS surface takes place successfully. In addition, absorption peaks at 2913 and 2976 cm^{-1} observed in the high-frequency region are ascribed to the asymmetric methylene and methyl symmetric stretches of stearic acid.[41]

X-rays diffraction analysis

Figures 3a to 3c reveal the XRD patterns of PAni, PAni/CS and PAni/CS/ZS coatings, respectively. XRD pattern of Fig. 3a represents a peak at 2θ value of 44° with plane (1, 1, 3) corresponding to α-Al_2O_3, and it has rhombohedral crystal structure. The peak at 65° with plane (3, 1, 4) corresponds to δ-Al_2O_3, and it has the tetragonal/primitive crystal structure.[42] The diffraction peak occurs at an angle 2θ = 16° with plane (0, 1, 0) and is due to the presence of benzenoid and quinoid ring in PAni chains.[43] Analyzing the diffraction peaks in Fig. 3b, the XRD pattern shows peaks at 2θ values 17° with plane (0, 2, 0), which correspond to CS.[44] In Fig. 3c, the observed diffraction peaks at 47.48° with plane (1, 0, 0) belong to the ZS (JCPDS # 00-055-1618).[45]

Mechanical properties of the coatings

The microhardness (Hv) and abrasion resistance of the PAni-, PAni/CS-, and PAni/CS/ZS-coated Al are shown in Figs. 4a and 4b. For the PAni- and PAni/CS-coated Al specimens, the Hv values are found to be 82.1 ± 12.35 and 97.2 ± 14.78, respectively. The Hv value (125.7 ± 13.42) obtained for the PAni/CS/ZS-coated Al is higher than that of the PAni- and PAni/CS-coated Al specimens. This may be due to the

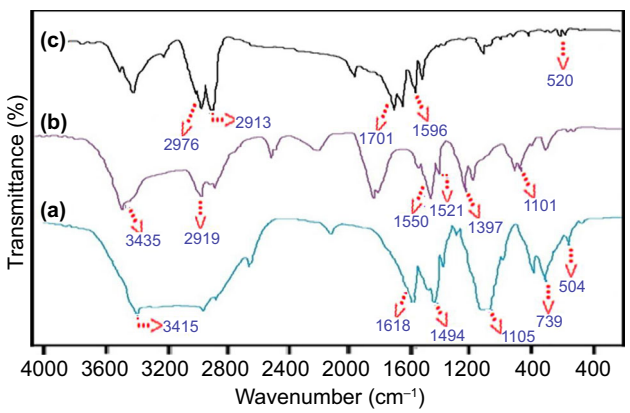

Fig. 2: ATR-IR spectra of (a) PAni. (b) PAni/CS. (c) PAni/CS/ZS coating on Al

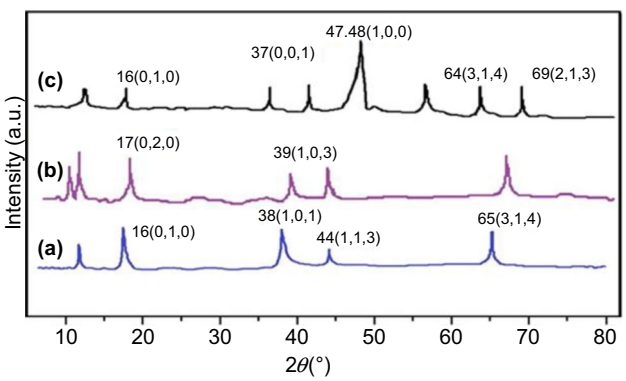

Fig. 3: XRD pattern of (a) PAni. (b) PAni/CS coating. (c) PAni/CS/ZS coating on Al

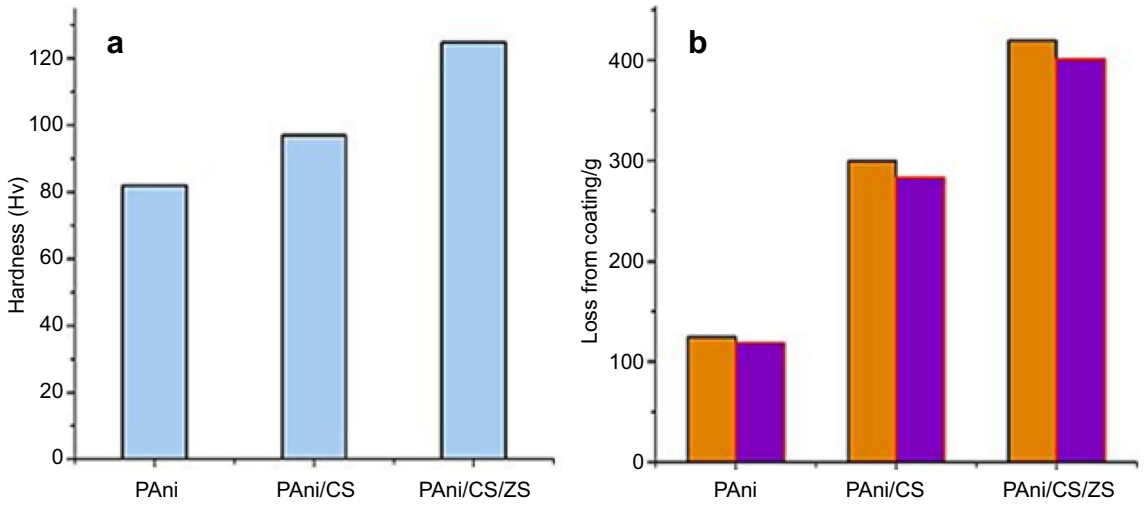

Fig. 4: (a) Hardness. (b) Abrasion resistance of various coatings on Al

inseparable bonding between PAni/CS and ZS superhydrophobic layer. The PAni, PAni/CS, and PAni/CS/ZS superhydrophobic-coated Al has the weight loss after abrasion test as 6 ± 2 μg, 17 ± 7 μg, and 30 ± 12 μg, respectively.

Surface morphology of coatings

Typical surface morphologies of PAni, PAni/CS, and PAni/CS/ZS superhydrophobic coatings are shown in Figs. 5a to 5c. Figure 5a shows the SEM image of the PAni coating on Al which has a clear smooth surface, but some pores are found in the surface morphology. Figure 5b represents an SEM image of the CS coating which has a rough surface and some cracks are found in that surface. The surface morphology PAni/CS coating is shown in Fig. 5c. The PAni/CS surface reveals a significant difference with monomer surfaces, and also it exhibits the uniform and compact surface without any cracks and pores. The PAni/CS film exhibits uniform coverage of passive film on Al surface, due to aggregation of PAni/CS on Al by continuous polymerization.[46–48]

It can be found from the SEM image of PAni/CS/ZS, Fig. 5d, that the surface is composed of a ball-flower-like structure. The higher magnification of Fig. 5f shows superhydrophobic surface consists of many 3D flower-like microclusters. Consequently, the flower-like hierarchical porous surface with a mass of channels or interspace is formed. In addition, the nanopores have an irregular structure, and a large fraction of air can be trapped in the pores. This morphology gives the super-repellent behavior. It is well known that the wettability of a solid depends on both the roughness and the chemical composition of the surface.[49,50] PAni/CS/ZS-coated on the Al surface has binary morphology with both a microscale and nanoscale structure and a number of low energy alkyl chains and that gives the excellent superhydrophobic property. Consequently, the resulting surface possesses a higher water contact angle (150.7°). Figure 5e shows the EDAX spectrum of the PAni/CS/ZS superhydrophobic coatings on Al specimen, which indicates the presence of C, Zn, N, Al, and O groups in the relative coating.

The root-mean-square (rms) roughness of the PAni, PAni/CS, and PAni/CS/ZS superhydrophobic coatings on Al specimen was measured as 92 nm, 174 nm, and 312 nm, respectively.

Contact angle measurement and surface energy of the fabricated coatings

Figures 6a and 6b illustrate the contact angle and surface energy of coatings. The contact angle of water on the PAni, PAni/CS, and PAni/CS/ZS coatings is $39° \pm 0.4°$, $24° \pm 0.2°$, and $150.7° \pm 0.7°$, respectively. The significant decrease in contact angles between PAni and PAni/CS, due to the presence of CS, and further increase of maximum contact angle 150.7° were observed on the high-adhesion of ZS on Al surface. The surface energies of PAni, PAni/CS, and PAni/CS/ZS superhydrophobic coatings are 49.3 ± 1.23 mJ/m^2, 45.2 ± 1.3 mJ/m^2, and 1.8 ± 1.1 mJ/m^2, respectively. From these values, it can be seen that the PAni/CS/ZS shows the lowest surface energy due to the presence of zinc stearate coating.

Evaluation of corrosion resistance of the various coatings

In order to evaluate the corrosion resistance of the PAni, PAni/CS, and PAni/CS/ZS superhydrophobic coatings, potentiodynamic polarization and electrochemical impedance spectroscopy were performed in 3.5% NaCl, respectively.

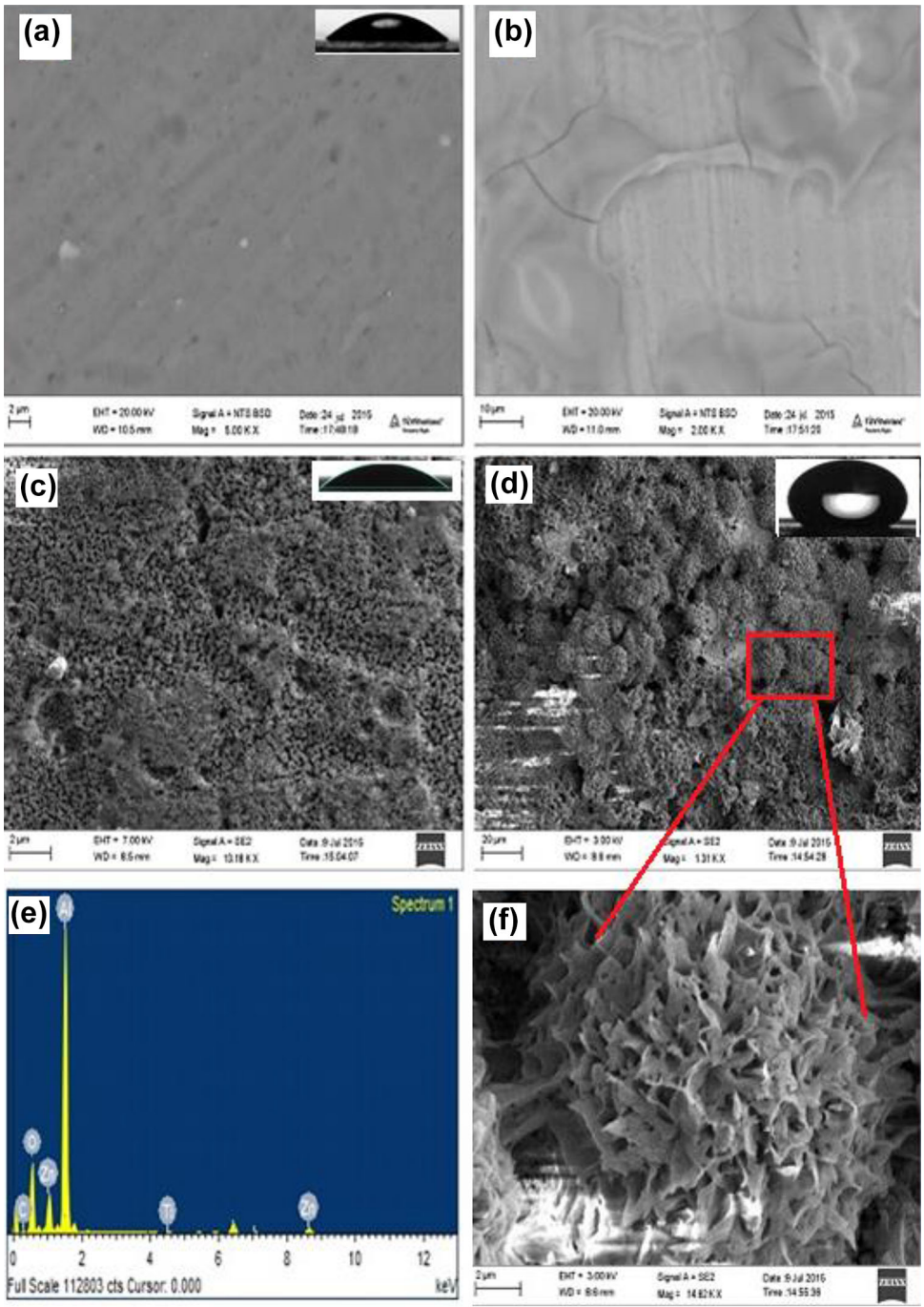

Fig. 5: FE-SEM images of (a) PAni. (b) CS. (c) PAni/CS. (d) PAni/CS/ZS. (e) EDX spectra of PAni/CS/ZS. (f) Higher-magnification PAni/CS/ZS coating on Al

Potentiodynamic polarization

The representative polarization curves for various polymer coatings are shown in Fig. 7. The parameters obtained by fitting the potentiodynamic curves are summarized in Table 1. Corrosion potential (E_{corr}) and corrosion current density (I_{corr}) were obtained by the Tafel extrapolation method. Cathodic/anodic Tafel constants (b_c and b_a) and polarization resistance (R_p) values were determined from Stern–Geary equation.[51]

$$R_p = b_a b_c / 2.303\, i_{corr}(b_a + b_c).$$

The corrosion rate was calculated using the following formula

$$CR = i_{corr} K \cdot EW/\rho A$$

where CR is corrosion rate (mils per year or mm per year, depending on units of K), K is constant for converting units, i_{corr} is corrosion current density (μA/cm^2 or A/cm^2), ρ is alloy density (g/cm^3), and EW is alloy equivalent weight (g/equiv).

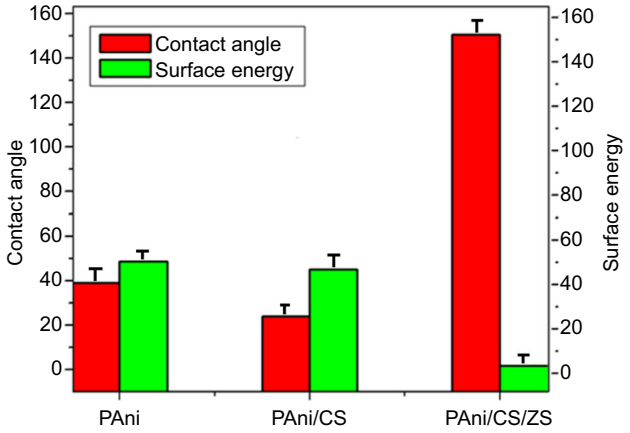

Fig. 6: Contact angle and surface energy of various coatings on Al

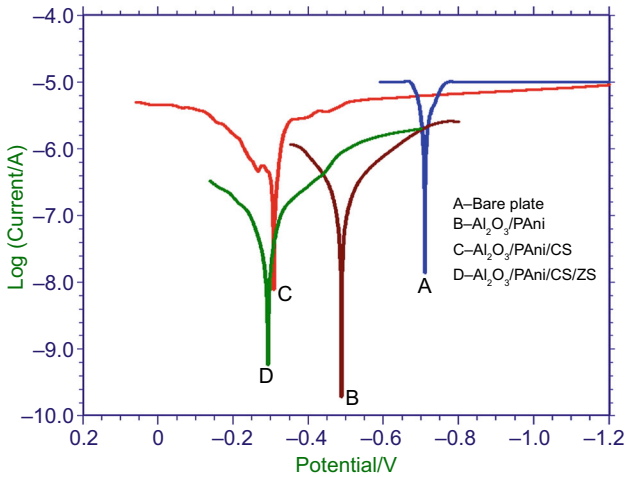

Fig. 7: Tafel polarization of various coatings on Al

The corrosion potential (E_{corr}) values of PAni/CS-coated Al are shifted to the positive direction compared to that of bare Al. The E_{corr} value is shifted from −0.832 V for bare Al to −0.488 V, −0.308 V for PAni- and PAni/CS-coated Al, respectively. The positive shift of E_{corr} further increased to −0.292 V for PAni/CS/ZS-coated Al. The I_{corr} values of various coatings decreased in the order PAni/CS/ZS < PAni/CS < PAni. From this, we can conclude that the PAni/CS/ZS coating has excellent corrosion resistance compared with all other coatings. The reason is as follows: PAni/CS inhibits corrosion by forming a compact barrier layer on Al, controlling both the anodic and cathodic reactions. In acidic solution, the PAni/CS molecules exist as protonated species. These protonated species are absorbed on the cathodic sites of Al surface and decrease the evolution of hydrogen. It is well known that the species have high molecular weight and bulky structure that cover the substrate uniformly and, also due to H-bonding between CS and PAni, the stability of the film is strong.[52] Corrosion protection is further increased due to the superhydrophobic surface, when ZS is added to PAni/CS. Here, the uniform rough surface is changed into a ball-flower-like micro–nanostructure which enhances the corrosion resistance. From a theoretical point of view, to increase corrosion resistance of an Al metal surface, it would be very effective to reduce the wetted area on a metal surface.[53] As mentioned, the air layer is stabilized within the grooves of the hierarchical superhydrophobic surface, and it reduces considerably the adsorption probability of aggressive (Cl^-) ions, resulting in an improvement in corrosion resistance.[54] Finally, based on the above results, we can conclude that the PAni/CS/ZS coating has better corrosion resistance than PAni/CS and PAni coatings.

EIS study of various coatings on Al substrate

EIS measurements were taken to confirm further coating performance and corrosion resistance of bare Al, PAni-, PAni/CS-, and PAni/CS/ZS-coated Al in 3.5% NaCl solution. It is clear from Table 1 that the charge transfer resistance (R_{ct}) value is increased from 5 cm^2 corresponding to bare Al to 493 KΩ·cm^2 for PAni coating. This is due to the metal corrosion and

Table 1: Electrochemical parameters of various coatings on Al substrate

Coatings	Corrosion potential/V versus SCE	Corrosion current/ μA/cm^2	Polarization resistance/ Ω cm^2	Corrosion rate/mpy	R_{ct}/kΩcm^2	C_{dl}/Ω Fcm^{-2}
Bare plate	−0.832	8.624×10^{-6}	9013.1	1.384×10^{1}	5.0	2.706×10^{-4}
PAni	−0.489	2.983×10^{-7}	134,627.1	2.623×10^{0}	493.8	1.563×10^{-5}
PAni/CS	−0.310	1.635×10^{-7}	261,842.7	1.388×10^{-1}	868.7	5.773×10^{-6}
PAni/CS/ZS	−0.292	8.653×10^{-8}	514,326.7	4.715×10^{-1}	1050	4.402×10^{-6}

the double layer capacitance (C_{dl}) of the liquid/metal interface, and then, the R_{ct} value is further increased to 869 KΩ·cm^2 for the PAni/CS coating. It may be due to the presence of PAni/CS on Al that its R_{ct} value is increased by the strongly oxidative property of the polymer.[55] In the anodic protection, the largest problem is the breakdown of a passive oxide due to the attack of aggressive anions such as chloride ions in solution and the breakdown is followed by a large damage of localized pitting corrosion and crevice corrosion.[56]

The R_{ct} value is further increased drastically to 1050 KΩ·cm^2 after ZS is coated on PAni/CS. Besides, the C_{dl} values are found to decrease considerably, which indicates the barrier effect of the superhydrophobic surface. This indicates that the superhydrophobicity plays an important role in improving the anticorrosion performance. It would be very effective to minimize the wetted area on the Al surface immersed in the aggressive solution. This surface has many roughness grooves like a nano-flower that could trap air at the solid–liquid interface. Therefore, the wetted area on a solid surface might be minimized if an air layer formed on the superhydrophobic surface that could be stabilized within the roughness groove.[57]

Similarly, EIS spectra in the form of Bode impedance plots and Bode phase angle plots recorded for various coated Al are given in Figs. 8a to 8c. Bode plots represent the relationship between phase angle and frequency. The bare Al shows the lesser phase angle when compared to other coatings. The phase angle maximum reaches 88° for PAni/CS/ZS, which suggests that this coating possesses higher corrosion resistance than other coatings. In the high-frequency region, EIS spectra of coated Al exhibited the coating behaviors, and in the low-frequency region, the spectra

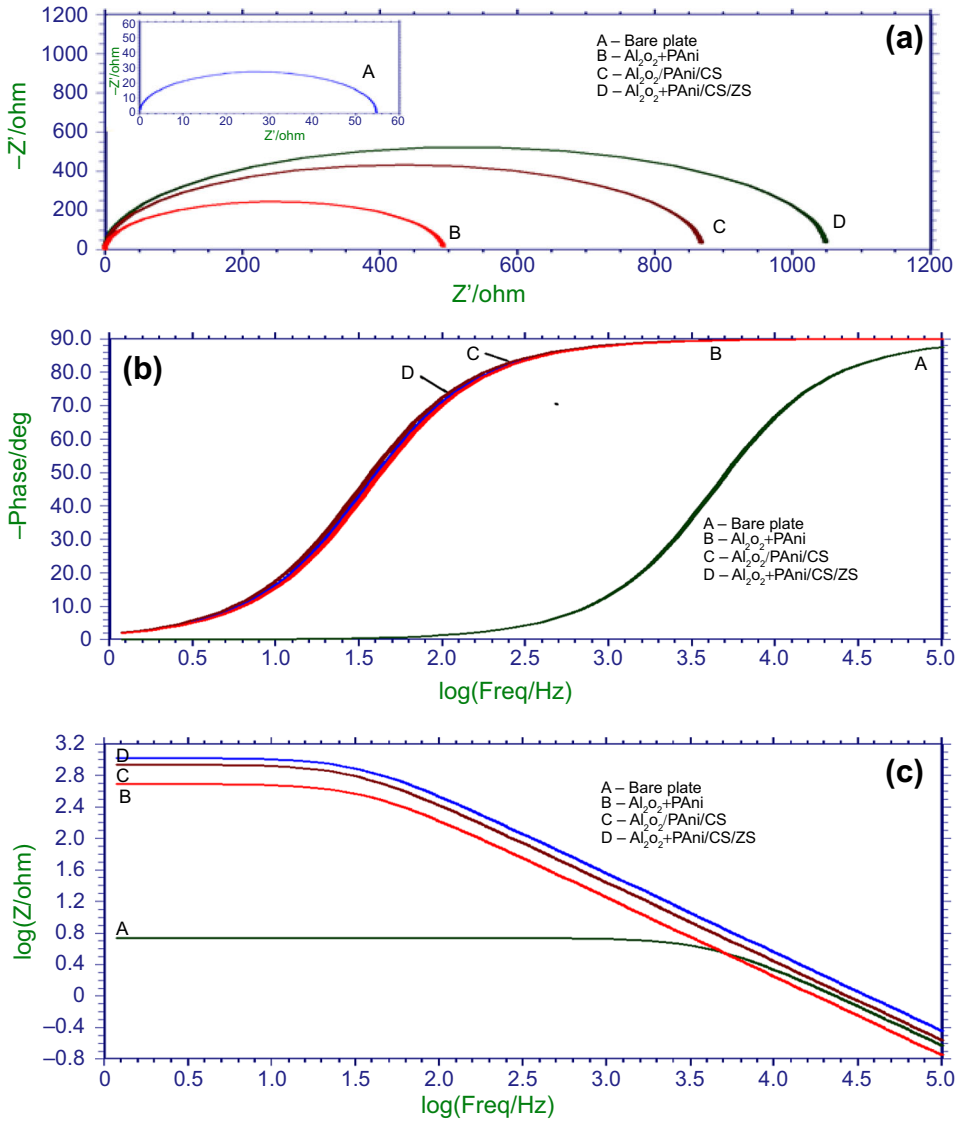

Fig. 8: (a) Nyquist plots. (b) Bode plots. (c) Phase plots of various coatings formed on Al

corresponded to corrosion reaction occurring on the metal under the coating. Thus, the superhydrophobic coating serves as an effective barrier against corrosion attack in the aggressive environment. The higher phase angle obtained may be strong oxidative property of the polymer and due to an area effect where the coating is blocking access of the aggressive electrolyte to the reactive Al surface.[58]

Antibacterial activity of various coatings

Bacterial adhesion on medical devices is the initial and crucial step for biofilm formation which leads to the failure of the function of the device. Bacterial adhesion is a complex process affected by many parameters such as crystallinity, charge and porosity of the surface type of bacteria, and environmental conditions.[59] The in vitro antibacterial activity of the samples was tested against two bacterial strains *S. aureus* and *E. Coli* by the agar disk diffusion method. Figure 9 shows the antibacterial activity of PAni, PAni/CS, and PAni/CS/ZS coatings against *S. aureus* and *E. coli* strains at 24 h, and its inhibition zone is shown in Fig. 10, which differs for different samples and organisms. The order of antibacterial activity of various coatings is PAni/CS/ZS > PAni/CS > PAni.

PAni/CS/ZS-coated Al has higher antibacterial activity against both the bacterial strains. This is because of the following: (1) due to their minimal solid–liquid contact at the surface, weak surface interactions with bacteria, and low surface energy molecule. As a result of these properties, it is energetically favorable for the bacteria to remain in solution and to roll off the surface instead of adhering to the superhydrophobic surface. (2) Zn is a well-known antibacterial agent over a wide spectrum of bacteria. The self-cleaning principle is the key to the antibacterial properties of superhydrophobic surface cleaned easily by simple rinsing, mitigating the need for antibacterial reagents.[60] Since this antibacterial design is purely structural, a product with permanent features can be fabricated for everyday use with minimal maintenance for the customer.

The reason for antibacterial activity of PAni/CS may be explained by the interaction between positively charged CS molecules and negatively charged microbial cell membranes, which may lead to leakage of

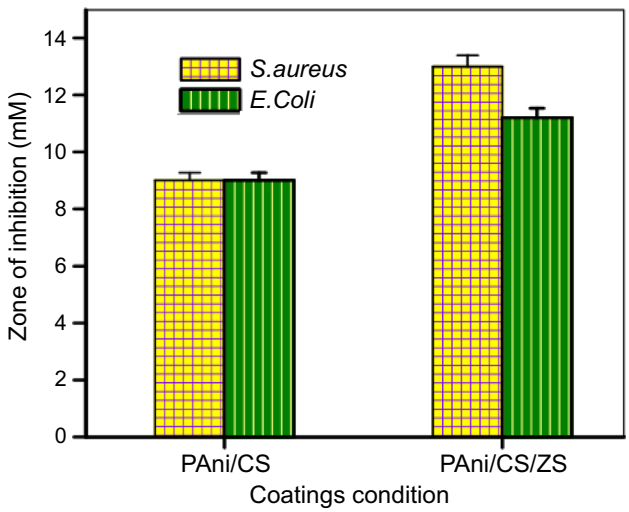

Fig. 10: Bar diagram of antibacterial activity of PAni, PAni/CS, PAni/CS/ZS coating against (a) *E. coli.* (b) *S. aureus*

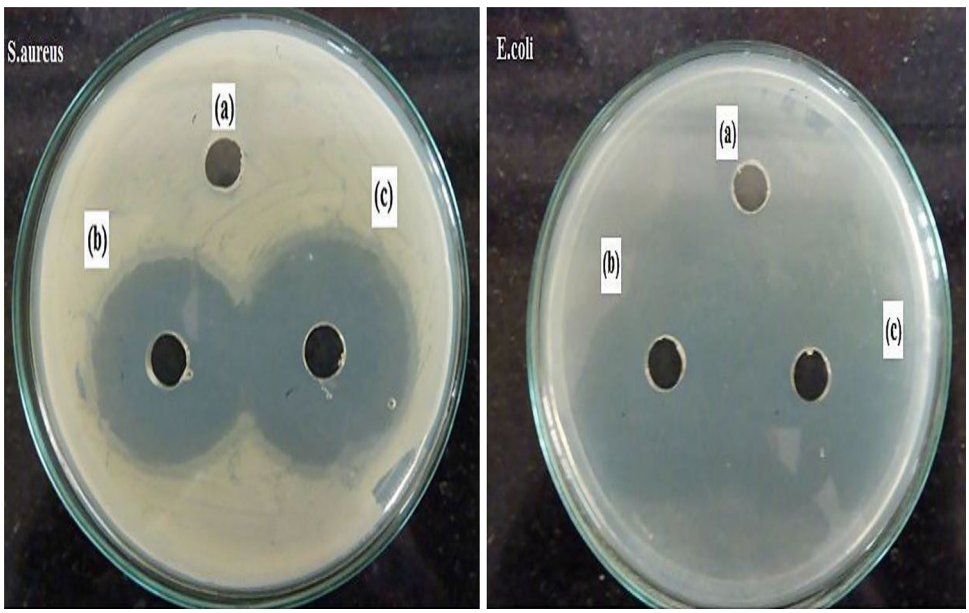

Fig. 9: Antibacterial activity of (a) PAni. (b) PAni/CS. (c) PAni/CS/ZS coating on Al

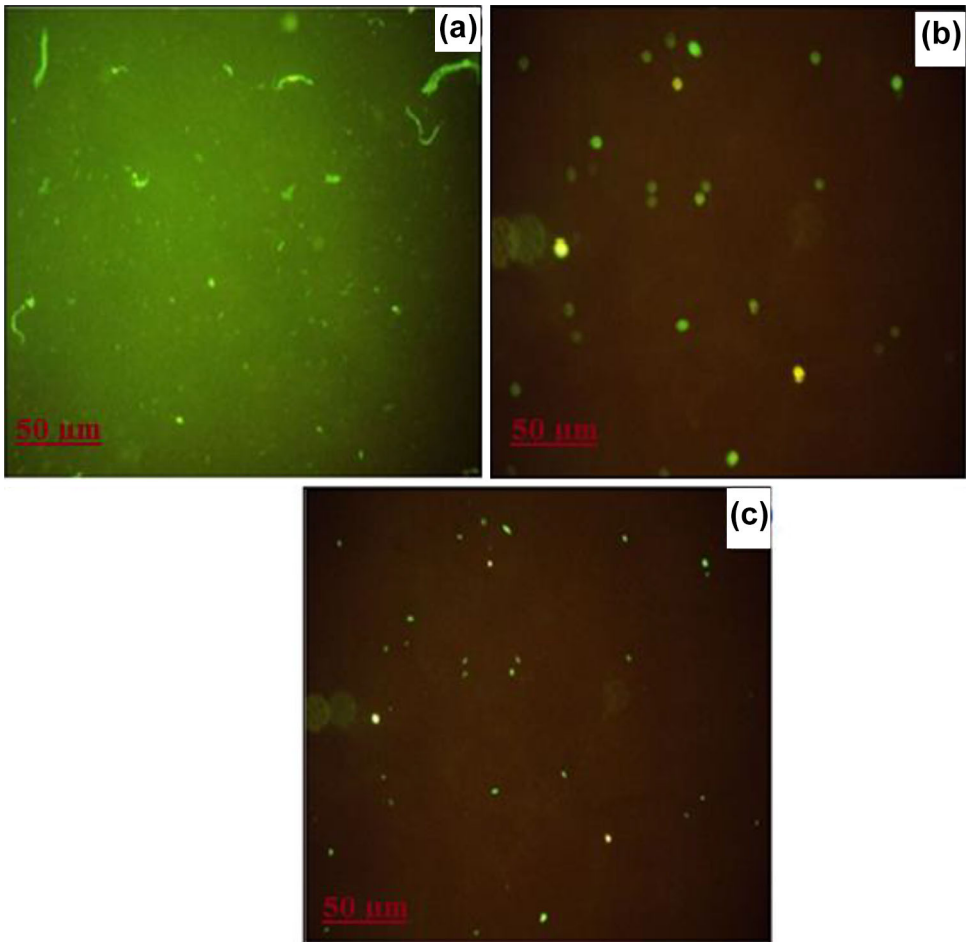

Fig. 11: Marine-bacterial activity of (a) PAni. (b) PAni/CS. (c) PAni/CS/ZS coating on Al

intracellular constituents of the bacteria, thus accelerating bacteria cells.[61]

Marine bacterial activity of various coatings on Al

The bacterial, antiadhesion activity of PAni, PAni/CS, PAni/CS/ZS coatings was tested against *Desulfovibrio desulfuricans* strains at 24 h, which is shown in Figs. 11a to 11c. Bacterial adhesion is higher in PAni and PAni/CS than in PAni/CS/ZS coating. This may be due to the hydrophilic nature of PAni and PAni/CS. After surface treatment with ZS, the surface changes from hydrophilic to superhydrophobic. So ZS-treated Al samples can resist the attachment of *Desulfovibrio desulfuricans* and have excellent MIC resistance properties, which can be attributed to the unique superhydrophobic surface of the PAni/CS/ZS-coated alumina. This superhydrophobic aliphatic carboxylate-treated surface has the potential to become an environmentally friendly MIC-resistant coating.[62] The strategy proposed in this work is simple, cheap, and allows for easy cleanup, and it has potential for commercial application in MIC protection.

Ice resistance ability of ZS coating on PAni/CS/Al

Ice resistance ability is an important property of superhydrophobic surfaces for their biomedical applications. Ice accretion has an enormous impact on transportation and energy production, electric power transmission and distribution (aluminum cables and towers).[63] An ice-phobic property of the as-prepared superhydrophobic surface was carried out by deliberately dipping it in rose colored water kept in a dish which was kept in the freezer (−4°C). Figure 12 (inset) shows the ice-phobic property of superhydrophobic surface, which was captured by a digital camera. There is no ice adhesion on superhydrophobic surface, due to the low energy of ZS-coated Al samples that can retain a very good superhydrophobicity even at −4°C, which greatly reduces the super-cooled water droplet to be adhered. So the obtained superhydrophobic aluminum surface can mitigate ice accretion. This may be (1) due to the low free energy of the surface modified by ZS, and the chemical bond between the surface and the water is not easily formed. When a water droplet touched the solid surface, the kinetic energy of the droplet is dissipated during the contact process. If the

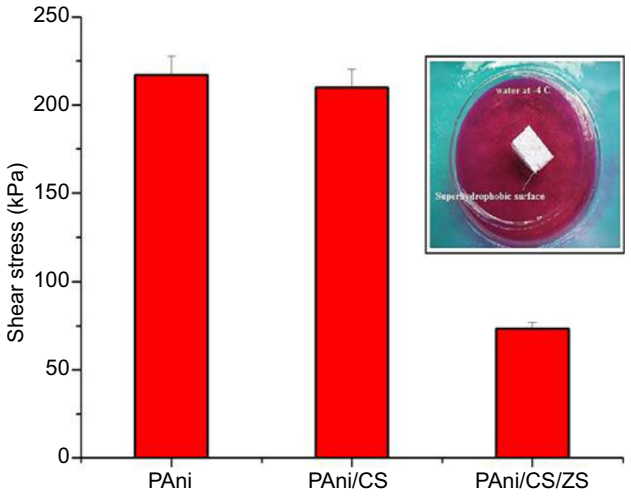

Fig. 12: Antiicing study of superhydrophobic coated on Al

energy dissipation is not too large, part of surface energy could revert to the kinetic energy and lead to retraction. The retraction process could mainly reflect the interaction between water droplets and the surface.[64] (2) The phenomenon is induced because of the nanostructure morphology on the ZS superhydrophobic coating surface, and the probable mechanical interlocking between the ice and the ZS superhydrophobic surface is trivial. From the ice resistance ability test, it can be assumed that decreasing wettability of the PAni/CS/ZS coating could minimize the surface accumulation of super-cooled water.[65]

For further study of ice adhesion property, the average shear stress values of bare Al, PAni-, PAni/CS-, and PAni/CS/ZS-coated Al are shown in Fig. 12. The results revealed a drastically reduced ice adhesion strength on the PAni/CS/ZS-coated Al. It may be due to a good combination of low surface energy, and micro–nano-scaled roughness resulting in an ice adhesion reduction and increased ice resistance ability.

Conclusion

A superhydrophobic surface with antiadhesion, antiicing, and anticorrosion properties was successfully fabricated on Al alloy by polymerization and electrodeposition. FE-SEM image shows that polyaniline/chitosan on aluminum surface yields a homogeneous rough surface, and after ZS addition, a ball-flower-like superhydrophobic surface was formed. It shows that dual morphology of the coatings consists of both microstructure and nanostructure with ca. 150.7°. The results of potentiodynamic polarization showed that the polyaniline/chitosan/zinc stearate superhydrophobic aluminum surface has an excellent corrosion resistance, and it could serve as an effective barrier against 3.5% NaCl solution. These fabricated superhydrophobic surfaces may be effective in eradicating SRB biofilms known to cause MIC in industrial field, and it inhibits bacterial colonization of medical implants. These coatings must also not pose significant cytotoxic effects to mammalian cells. These biocompatible polymers can be used as antiadhesive to osteoblasts in addition to the bacteria. Such a facile and low-cost method could be easily applied to large-scale productions of superhydrophobic anticorrosion aluminum alloy surfaces.

Acknowledgments We acknowledge the major financial support from the Department of Science and Technology, New Delhi, India (DST-SERB, Ref. No.: SERB/F/7154/2013-14).

References

1. Martin, CR, ''Membrane-based Synthesis of Nanomaterials.'' *Chem. Mater.,* **8** 1739–1746 (1996)
2. Tiruvenkadam, N, Thyla, PR, Senthilkumar, M, Bharathiraja, M, Murugesan, A, ''A Synthesis of New Aluminum Nano Hybrid Composite Liner for Energy Saving in Diesel Engines.'' *Energy Convers. Manag.,* **98** 440–448 (2015)
3. Li, Y, Burstein, GT, Hutchings, IM, ''The Influence of Corrosion on the Erosion of Aluminium by Aqueous Silica Slurries.'' *Wear,* **186** 515–522 (1995)
4. Rao, TS, ''Combating Bacterial Colonization on Metals via Polymer Coatings.'' *Corros. Rev.,* **22** 333–365 (2009)
5. Beech, I, Sunner, B, ''Biocorrosion: Towards Understanding Interactions Between Biofilms and Metals.'' *J. Curr. Opin. Biotechnol.,* **15** 181–186 (2004)
6. Feng, L, Song, Y, Zhai, J, Liu, B, Jiang, L, Zhu, D, ''Creation of a Super Hydro Phobic Surface from an Amphiphilic Polymer.'' *Angew. Chem. Int. Edition,* **42** 800–802 (2003)
7. Kalaivasan, N, Syed Shafi, S, ''Synthesis of Various Polyaniline/Clay Nanocomposites Derived from Aniline and Substituted Aniline Derivatives by Mechanochemical Intercalation Method.'' *E J. Chem.,* **7** 1477–1483 (2010)
8. Narayanan, BN, Koodathil, R, Gangadharan, T, Yaakob, Z, Saidu, F, Handralayam, S, ''Preparation and Characterization of Exfoliated Polyaniline/Montmorillonite Nanocomposites.'' *Mater. Sci. Eng. B*, **168** 242–244 (2010)
9. Baldissera, AF, Ferreira, CA, ''Coatings Based on Electronic Conducting Polymers for Corrosion Protection of Metals.'' *Prog. Org. Coat.,* **75** 241–247 (2012)
10. Tanveer, N, Mobin, M, ''Anti-corrosive Properties of Poly(2-pyridylamine-coaniline-co-2, 3-xylidine) Terpolymer Coating on Mild Steel in Different Corrosive Environments.'' *Prog. Org. Coat.,* **75** 231–240 (2012)
11. Nagels, GT, Winand, R, Weymeersch, A, Renard, L, ''Electron Conducting Organic Coating of Mild Steel by Electropolymerization.'' *J. Appl. Electrochem.,* **22** 756–764 (1992)
12. Sekine, I, Kohara, K, Sugiyama, T, Yuasa, M, ''Syntheses of Polymerized Films on Mild Steels by Electro-Oxidation and Electroreduction and Their Corrosion Resistance.'' *J. Electrochem. Soc.,* **139** 3090–3097 (1992)
13. Kamaraj, K, Karpakam, V, Sathiyanarayanan, S, Venkatachari, G, ''Electrosysnthesis of Poly(aniline-co-m-amino benzoic acid) for Corrosion Protection of Steel.'' *Mater. Chem. Phys.,* **122** 123–128 (2010)
14. Wei, Y, Hariharan, R, Patel, S, ''Chemical and Electrochemical Copolymerization of Aniline with Alkyl Ring-Substituted Anilines.'' *Macromolecules,* **23** 758–764 (1990)

15. Chen, CX, Gao, YH, ''Electrochemical Characteristics of Polyaniline Electro-Synthesized in the Presence of Neutral Red.'' *Mater. Chem. Phys.,* **102** 24–30 (2007)
16. Rhazi, M, Desbrieres, J, Tolaimate, A, Alagui, A, Vottero P, ''Investigation of Different Natural Sources of Chitin: Influence of the Source and Deacetylation Process on the Physicochemical Characteristics of Chitosan.'' *Polym. Int.,* **49** 337–344 (2000)
17. Yalcınkaya, S, Demetgul, C, Colak, N, ''Electrochemical Synthesis and Characterization of Polypyrrole/Chitosan Composite on Platinum Electrode: Its Electrochemical and Thermal Behaviors.'' *Carbohydr. Polym.,* **79** 908–913 (2010)
18. Wallace, G, Smyth, M, Zhao, H, ''Conducting Electroactive Polymer-Based Biosensors.'' *Trends Anal. Chem.,* **18** 245–251 (1999)
19. Lundvall, O, Gulppi, M, Paez, MA, Gonzalez, E, Zagal, JH, Pavez, J, Thompson, GE, ''Copper Modified Chitosan for Protection of AA-2024.'' *Surf. Coat. Technol.,* **201** 5973–5978 (2007)
20. Alsabagh, M, Elsabee, MZ, Moustafa, YM, Elfky, A, Morsi, RE, ''Corrosion Inhibition Efficiency of Some Hydrophobically Modified Chitosan Surfactants in Relation to Their Surface Active Properties.'' *Egypt. J. Petrol.,* **23** 349–359 (2014)
21. Meruvu, H, Vangalapati, M, Chaitanya Chippada, S, Bammidi, S, ''Synthesis and Characterization of Zinc Oxide Nanoparticles and Its Antimicrobial Activity Against *Bacillus subtilis* and *Escherichia coli*.'' *Rasayan J. Chem.,* **4** 217–222 (2011)
22. Ning, T, Xu, WG, Lu, SX, ''Fabrication of Superhydrophobic Surfaces on Zinc Substrates and Their Application as Effective Corrosion Barriers.'' *Appl. Surf. Sci.,* **258** 1359–1365 (2011)
23. Yuan, SJ, Pehkonen, SO, Liang, B, Ting, YP, Neoh, KG, Kang, ET, ''Super Hydrophobic Fluoropolymer-Modified Copper Surface via Surface Graft Polymerisation for Corrosion Protection.'' *Corros. Sci.,* **53** 2738–2747 (2011)
24. Li, J, Liu, X, Ye, Y, Zhou, H, Chen, J, ''A Simple Solution-Immersion Process for the Fabrication of Superhydrophobic Cupric Stearate Surface with Easy Repairable Property.'' *Appl. Surf. Sci.,* **258** 1772–1775 (2011)
25. Escobar, M, Llorca-Isern, N, ''Superhydrophobic Coating Deposited Directly on Aluminum.'' *Appl. Surf. Sci.,* **305** 774–782 (2014)
26. Kwak, G, Seol, M, Tak, Y, Yong, K, ''Superhydrophobic ZnO Nanowire Surface: Chemical Modification and Effects of UV Irradiation.'' *J. Phys. Chem. C,* **113** 12085–12089 (2009)
27. Qian, B, Shen, Z, ''Fabrication of Superhydrophobic Surfaces by Dislocation-Selective Chemical Etching on Aluminum, Copper, and Zinc Substrates.'' *Langmuir,* **21** 9007–9009 (2005)
28. Song, JL, Xu, WJ, Lu, Y, ''One-Step Electrochemical Machining of Superhydrophobic Surfaces on Aluminum Substrates.'' *J. Mater. Sci.,* **47** 162–168 (2012)
29. Zaraska, L, Sulka, GD, Jaskuła, M, ''The Effect of n-Alcohols on Porous Anodic Alumina Formed by Self-organized Two-Step Anodizing of Aluminum in Phosphoric Acid.'' *Surf. Coat. Technol.,* **204** 1729–1737 (2010)
30. Owens, DK, Wendt, RC, ''Estimation of the Surface Free Energy of Polymers.'' *J. Appl. Polym. Sci.,* **13** 1741–1747 (1969)
31. Carre, A, ''Polar Interactions at Liquid/Polymer Interfaces.'' *J. Adhes. Sci. Technol.,* **21** 961–981 (2007)
32. Zinkevich, V, Bogdarina, I, Kang, H, Hill, MA, Tapper, R, Beech, IB, ''Characterization of Exopolymers Produced by Different Isolates of Marine Sulfate Reducing Bacteria.'' *Int. Biodeterior. Biodegrad.,* **37** 63–69 (1996)
33. Salsvagiona, HI, Miras, MC, Barbero, C, ''Chemical Lithography of a Conductive Polymer Using a Traceless Removable Group.'' *J. Am. Chem. Soc.,* **25** 5290–5296 (2003)
34. Kamaraj, K, Sathiyanarayanan, S, Muthukrishnan, S, Venkatacahari, G, ''Corrosion Protection of iron by Benzoate Doped Polyaniline Containing Coatings.'' *Prog. Org. Coat.,* **64** 460–465 (2009)
35. Jhansen, HD, Brett, CMA, Motheo, AJ, ''Corrosion Protection of Aluminium Alloy by Cerium Conversion and Conducting Polymer Duplex Coatings.'' *Corros. Sci.,* **63** 342–350 (2012)
36. Chakradhar, RP, Dinesh Kumar, V, ''Water-Repellent Coatings Prepared by Modification of ZnO Nanoparticles.'' *Spectrochim. Acta,* **94** 352–356 (2012)
37. Sedaghat, S, ''Synthesis and Characterization of New Bio Compatible Copolymer: Chitosan Graft Polyaniline.'' *Int. Nano Lett.,* **4** 2–9 (2014)
38. Khan, R, Dhayal, M, ''Chitosan/Polyaniline Hybrid Conducting Biopolymer Base Impedi Metric Immunosensor to Detect Ochratoxin-A.'' *Biosens. Bioelectron.,* **24** 1700–1705 (2009)
39. Salavagione, HJ, Acevedo, DF, Miras, AC, Motheo, AJ, Barbero, CA, ''Comparative Study of 2-Amino and 3-Aminobenzoic Acid Copolymerization with Aniline Synthesis and Copolymer Properties.'' *J. Polym. Sci. A Polym. Chem.,* **42** 5587–5599 (2004)
40. Cansen, L, Fenghua, S, Jizhao, L, Huang, P, ''Facile Fabrication of Superhydrophobic Cerium Coating with Micro-nano Flower-Like Structure and Excellent Corrosion Resistance.'' *Surf. Coat. Technol.,* **258** 580–586 (2014)
41. Zhi-feng, L, Peng, W, Dun, Z, Yi, W, ''A ZnO/Chitosan Composite Film: Fabrication and Anticorrosion Characterization.'' *Adv. Mater. Res.,* **153** 1199–1202 (2011)
42. Raj, V, Mumjitha, M ''Comparative Study of Formation and Corrosion Performance of Porous Alumina and Ceramic Nanorods Formed in Different Electrolytes by Anodization.'' *Mater. Sci. Eng. B,* **179** 25–35 (2014)
43. Mostafaei, A, Zolriasatei, A, ''Synthesis and Characterization of Conducting Polyaniline Nanocomposites Containing ZnO Nanorods.'' *Prog. Nat. Sci. Mater. Int.,* **22** 273–280 (2012)
44. John, S, Joseph, A, Joes, AJ, ''Enhancement of Corrosion Protection of Mild Steel by Chitosan/ZnO Nanoparticle Composite Membranes.'' *Prog. Org. Coat.,* **84** 28–34 (2015)
45. Wang, S, Feng, L, Jiang, L, ''One-Step Solution-Immersion Process for the Fabrication of Stable Bionic Superhydrophobic Surfaces.'' *Adv. Mater.,* **18** 767–770 (2006)
46. Thiemann, C, Brett, C, ''Electrosynthesis and Properties of Conducting Polymers Derived from Amino Benzoic Acid and Aniline.'' *Synth. Metals,* **123** 1–7 (2001)
47. Ohsaka, T, Ohnuki, Y, Oyama, N, Katagiri, G, Kamisako, K, ''IR Absorption Spectro Scopic Identification of Electroactive and Electroinactive Polyaniline Films Prepared by the Electrochemical Polymerization of Aniline.'' *J. Electroanalyt. Chem.,* **161** 399–405 (2001)
48. Nunziante, P, Pistoia, G, ''Factors Affecting the Growth of Thick Polyaniline Films by the Cyclic Voltammetry Technique.'' *Electrochim. Acta,* **34** 223–229 (1989)
49. Feng, LB, Che, YH, ''Superhydrophobic Alumina Surface Based on Stearic Acid Modification.'' *Appl. Surf. Sci.,* **283** 367–374 (2013)
50. Al-Qadhi, M, Merah, N, Matin, A, Abu-Dheir, N, Khaled, M, Youcef-Toumi, K, ''Preparation of Superhydrophobic and Self-cleaning Polysulfone Non-wovens by Electrospinning: Influence of Process Parameters on Morphology and Hydrophobicity.'' *Polym. Res.,* **22** 207–212 (2015)

51. Stern, M, Geary, AL, ''Electrochemical Polarization I, A Theoretical Analysis of the Shape of Polarization Curves.'' *J. Electrochem. Soc.,* **104** 56–63 (1957)
52. Siva, T, Kamaraj, K, Sathiyanarayanana, S, ''Electrosynthesis of Poly (aniline-co-o-phenyl enediamine) Film on Steel and Its Corrosion Protection Performance.'' *Prog. Org. Coat.,* **77** 1807–1815 (2014)
53. Wang, P, Zhang, D, Qiu, R, Hou, B, ''Super-Hydrophobic Film Prepared on Zinc as Corrosion Barrier.'' *Corros. Sci.,* **3** 2080–2086 (2011)
54. Mostafaei, A, Zolriasatein, A, ''Synthesis and Characterization of Conducting Polyaniline Nanocomposites Containing ZnO Nanorods.'' *Mater. Int.,* **22** 273–280 (2012)
55. Ohtsuka, T, ''Corrosion Protection of Steels by Conducting Polymer Coating.'' *Int. J. Corros.,* **12** 1–7 (2012)
56. Madhankumar, A, Rajendran, N, ''Influence of Zirconia Nanoparticles on the Surface and Electrochemical Behaviour of Polypyrrole Nanocomposite Coated 316L SS in Simulated Body Fluid.'' *Surf. Coat. Technol.,* **213** 155–166 (2012)
57. Phanasgaonkar, A, Raja, VS, ''Influence of Curing Temperature, Silica Nanoparticles- and Cerium on Surface Morphology and Corrosion Behaviour of Hybrid Silane Coatings on Mild Steel.'' *Surf. Coat. Technol.,* **203** 2260–2271 (2009)
58. Mansfeld, F, ''Use of Electrochemical Impedance Spectroscopy for the Study of Corrosion by Polymer Coatings.'' *J. Appl. Electrochem.,* **25** 187–202 (1995)
59. Huo, K, Zhang, X, Wang, H, Zhao, L, Liu, X, Chu, PK, ''Osteogenic Activity and Antibacterial Effects on Titanium Surfaces Modified with Zn-incorporated Nanotube Arrays.'' *Biomaterials,* **34** 3467–3478 (2013)
60. Premanathan, M, Krishnamoorthy, K, Jeyasubramanian, K, Manivannan, G, ''Selective Toxicity of ZnO Nanoparticles Toward Gram-Positive Bacteria and Cancer Cells by Apoptosis Through Lipid Peroxidation.'' *Nanomed. Nanotechnol. Biol. Med.,* **7** 184–189 (2011)
61. Kompany, E, Mirza, H, Hosseini, S, Murphy, BP, Djordjevic I, ''Polyoctanediol Citrate–ZnO Composite Films: Preparation, Characterization and Release Kinetics of Nanoparticles from Polymer Matrix.'' *Mater. Lett.,* **126** 165–168 (2014)
62. Ferrari, M, Benedetti, A, Santini, E, Liggieri, L, Guzman, E, Cirisano, F, ''Physico Chemical and Engineering Aspects Biofouling Control by Superhydrophobic Surfaces in Shallow Euphotic Seawater.'' *Colloids Surf. A Physicochem. Eng. Asp.,* **480** 369–375 (2015)
63. Li, X, Zhang, K, Zhao, Y, Zhu, K, Yuan, X, ''Formation of Icephobic Film from POSS-Containing Fluorosilicone Multiblock Methacrylate Copolymers.'' *Prog. Org. Coat.,* **89** 150–159 (2015)
64. Wang, Y, Xue, J, Wang, Q, Chen, Q, Ding, JF, ''Verification of Icephobic/Anti-icing Properties of a Superhydrophobic Surface.'' *ACS Appl. Mater. Interfaces,* **5** 3370–3381 (2013)
65. Bahadur, V, Mishchenko, L, Hatton, B, Taylor, JA, Aizenberg, J, Krupenkin, T, ''Predictive Model for Ice Formation on Superhydrophobic Surfaces.'' *Langmuir,* **27** 14143–14150 (2011)